ARCTIC — IN PRESS
https://doi.org/10.14430/arcticxxxxx

Monitoring Lake Ice and Snow in the Canadian High Arctic Using Digital Camera Imagery

Brianna E. Lane[1] and Laura C. Brown[1,2]

(*Received 4 October 2025; accepted in revised form 5 March 2026*)

ABSTRACT. In the Arctic region, a decline in ice and snow cover has been observed in recent years, resulting in adverse effects on the climate, hydrological events, biological processes, and human populations. Monitoring changes in ice and snow cover using satellite imagery or models is common, while novel research is beginning to use ground-based camera systems for in situ monitoring of cryosphere elements. This study focused on maximizing the usage of ground-based time-lapse imagery from trail cameras for ice and snow studies from 2016-2022 within the context of the changing Arctic climate by monitoring lake ice and snow at five lakes (Resolute Lake, Small Lake, North Lake, Plateau Lake, and Hunting Camp Lake) near Resolute and Nanuit Itillinga, Nunavut, in the Central Canadian High Arctic. A semi-automated technique using image classification tools was developed to quantify the progression of ice and snow extent in the camera view. The image classification yielded an overall classification accuracy of 86%, and a Kappa coefficient of 0.79 from nearly 13 000 images, indicating a strong and viable monitoring system despite some variance in performance from viewing conditions. Lake ice and snow phenology dates determined from classified imagery had averages generally within a few days of observations (mean bias error of 2-9 days). Average ice duration was 308 days (September 20 to July 25), and average snow duration was 298 days (September 14 to July 8). The camera-based data extraction technique is a viable tool, not only for tracking long-term changes in snow/ice conditions, but also for validating satellite or modelling work in other logistically challenging environments. Thus, this methodology to monitor Arctic ice and snow phenology can support better projections for future responses to climate change.

Keywords: Lake Ice; Snow; digital imagery; trail cameras; image classification

[1] Department of Geography, Geomatics and Environment, University of Toronto Mississauga, 3359 Mississauga Road, Mississauga, Ontario L5L 1CG, Canada
[2] Corresponding author: lc.brown@utoronto.ca

INTRODUCTION

The rapid warming of the Arctic is an increasing concern. Currently, the Arctic region is warming at a rate four times the global average since 1979 (Rantanen et al., 2022), resulting in a decline in both the extent and duration of ice and snow in recent years (Wang et al., 2022; Young, 2023). This loss has negative implications for areas such as the global climate due to feedbacks from decreased surface reflectivity (albedo) (Brown and Duguay, 2010; Young, 2023); hydrological events such as timing of melt and freeze (Geldsetzer et al., 2010); lake ecology, including species' habitat conditions and interactions (Hampton et al., 2017); and human communities that face hazards for key transportation routes and recreational activities (Brown and Duguay, 2010).

Lake ice duration is projected to decrease considerably by the end of the century (Huang et al., 2022). Other phenological changes include later freeze-up and earlier break-up in the Northern Hemisphere (e.g., Benson et al., 2012; Dauginis and Brown, 2021). One study recorded greater changes in far northern lakes compared to other Canadian lakes, specifically later freeze-up (Latifovic and Pouliot, 2007), highlighting the need for increased focus on northern sites. Snow cover is expected to follow similar trends, with projections estimating that by the end of the century, rain will become the dominant form of precipitation in the Arctic (McCrystall et al., 2021). Additionally, recent studies indicate that the timing of snow cover is already shifting in the Canadian Arctic (e.g., Dauginis and Brown, 2021), and decreases in spring snow cover extents have been reported across the pan-Arctic and Northern Hemisphere (Mudryk et al., 2020, 2022). Therefore, monitoring snow and ice is crucial due to the interconnected nature of the Arctic system.

Over the past forty years, there has been a decline in ground-based lake ice monitoring in Canada (Lenormand et al., 2002) and other pan-Arctic countries (Prowse et al., 2011; Murfitt and Duguay, 2021), with spatial coverage and representation particularly limited in the Canadian Arctic. Similarly, snow cover observations, including measurements of snow water equivalent and precipitation, are restricted by spatial and temporal gaps (Bokhorst et al., 2016).

Logistical challenges (such as inaccessibility and remoteness) and harsh environmental conditions in the Arctic promote the use of satellite imagery and modelling (e.g., Arp et al., 2010; Du et al., 2017; MacKay et al., 2017; Zhang et al., 2021), which can be valuable for extensive monitoring. However, despite the many applications of off-site methods, the necessity for observation-based ground data to validate satellite imagery and modelling data still remains.

Previous research has documented the extent and coverage of lake ice and snow using satellite imagery and model-based approaches (e.g., Brown and Duguay, 2010). While satellite data can be limited by spatial and temporal resolution (Xiao et al., 2018), innovative research is starting to make use of digital camera imagery for in situ monitoring, such as using automated cameras to study changing lake and river ice (Ansari et al., 2017; Xiao et al., 2018; Ariano and Brown, 2019). Ground-based cameras are relatively affordable, straightforward to install, and generally offer higher resolution than space-based platforms (Xiao et al., 2018), enabling detection of subtle regional variations (e.g., ice and snow redistribution on smaller lakes). However, previous studies using ground-based cameras for monitoring have faced challenges during the freeze/melt transition when lakes are only partially frozen (Xiao et al., 2018) and in applying methods across different lakes (Tom et al., 2020).

Landcover classification is a widely used tool in remote sensing. Earlier research in northern Canada has explored various classification techniques to evaluate land cover in relation to ecological structure and to classify ecosystems (Atkinson and Treitz, 2012; Chasmer et al., 2014; Bothmann et al., 2017; Hung and Treitz, 2020). While landcover classification remains popular for ecological studies in the Canadian Arctic, fewer investigations have focused on lake ice through image classification for cryosphere monitoring. Examples include supervised classification of lake ice cover at the Great Lakes in Canada (Leshkevich and Nghiem, 2013), the application of a random forest machine learning algorithm at Qinghai Lake in China (Han et al., 2020) and employing random forest classifiers to track lake ice from MODIS data globally (Wu et al., 2021). Remote sensing already offers a valuable method for monitoring lake ice and snow (e.g., Murfitt and Duguay, 2021, Mudryk et al., 2020), and there is great potential to extend this approach with ground-based cameras and broaden it to other cryosphere observations. The objectives of this research were to develop a feasible method for extracting ice and snow phenology from a large volume of in situ digital imagery and to validate this new approach against manually extracted snow and ice phenology from the imagery, assessing its accuracy and practicality for studying recent phenological changes in the Central Canadian High Arctic.

METHODOLOGY

Study Area

Field research was carried out on five lakes in the Central Canadian High Arctic: Resolute Lake, Small Lake, North Lake, and Plateau Lake near the community of Resolute or Qausuittuq, NU (74˚ 43'N, 94˚ 58'W) on the southern coast of Cornwallis Island, along with Hunting Camp Lake in Nanuit Itillinga (formerly Polar Bear Pass) National Wildlife Area (75˚ 44'N, 98˚ 25'W) on Bathurst Island (**Fig. 1**). This study area is a low-elevation polar desert ecoregion with limited vegetation growth (French and Slaymaker, 2011; Young et al., 2018). Based on data from 1991 to 2020, the daily average temperatures in Resolute are 4.9˚C in July and -32.1˚C in February, the warmest and coldest months,

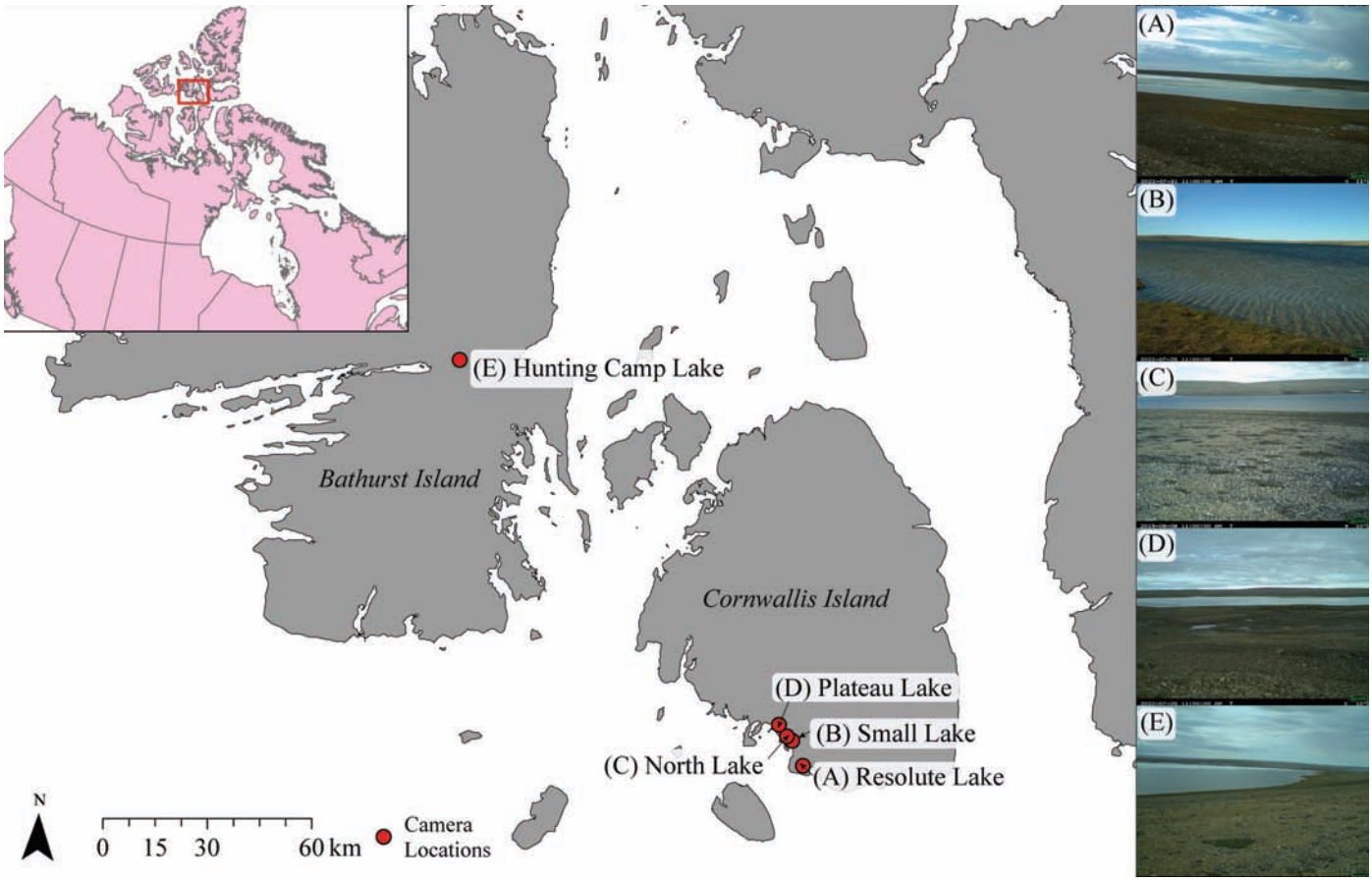

FIG. 1. Location of field sites on Bathurst Island and Cornwallis Island. Red markers represent the location of the cameras. An example of digital imagery from each camera is given on the right for (a) Resolute Lake, (b) Small Lake, (c) North Lake, (d) Plateau Lake, and (e) Hunting Camp Lake. Base map source: Statistics Canada. https://www12.statcan.gc.ca/census-recensement/2011/geo/bound-limit/bound-limit-2016-eng.cfm

respectively (ECCC, 2022). Precipitation mainly falls as snow (about 100 cm annually), with around 60 mm of rain each year, and little precipitation occurs between November and April (ECCC 2022). Nanuit Itillinga, where Hunting Camp Lake is located, has been identified as having overall similar weather and climate conditions to Resolute, despite being a polar semi-dessert (Young and Labine, 2010). The terrain surrounding the wetlands varies in elevation from 23 m to 180 m above sea level (Young and Labine, 2010; Young, 2019).

Methods

A series of Reconxy HyperFire Outdoor Cameras (PC800 HyperFire Professional IR and HyperFire 2 Professional HP2X) were previously installed, with one camera overlooking each of the five lakes (**Table 1**). The captured imagery spans a period of two to seven years (2016-2022) and mostly consists of images taken twice daily at 11:00 a.m. and 1:00 p.m. Central Standard Time (CST) (**Table 2**). These times were selected to optimize visibility as the day length shortens before the onset of polar night, the period of twenty-four-hour darkness in winter. Exceptions include Resolute Lake, where images are taken once daily at 1 pm CST from June 6, 2018, onwards, and Plateau Lake and North Lake, where extra images were collected during the first phenological year of data collection (2019-2020), with images taken on the hour from 6 am CST to 6 pm CST, though these additional images were only used as supplementary information. All cameras were installed in locations that afforded the best possible visibility of the lakes, based on accessibility (Ariano and Brown, 2019), following consultation with local representatives from the Resolute community. They were secured to rebar with cold-weather (-40˚C) zip-ties to ensure they remained stable through inclement weather and winter conditions (**Fig. 2**). The cameras are approximately 70 cm high, chosen to minimize snow coverage on the lens while reducing wind interference common with taller poles. Duct seal putty was applied around each camera for added weatherproofing, and a protective casing was placed around the battery wire to limit power disruptions caused by wildlife chewing wires. Power was supplied by an external12-volt battery housed in a weatherproof box, covered with rocks for extra protection, with internal AA lithium batteries serving as backup in case the external power failed (one camera is powered solely by AA batteries).

Ground-truthing surveys were conducted during the summers of 2021 and 2022. Ground truthing was conducted at Resolute Lake on August 12, 2021, with ten ground

TABLE 1. The location of each camera and the corresponding lake characteristics. All sites are in Nunavut, Canada.

Lake name	Location	Latitude	Longitude	Elevation (m a.s.l.)	Camera orientation	Surface area (km^2)	Maximum depth (m)	Mean depth (m)
Resolute Lake	Cornwallis Island	74.72˚N	94.95˚W	1.49	SE	1.27	22.5	7.9
Small Lake[1]	Cornwallis Island	74.76˚N	95.06˚W	18.52	W–SW	0.2*	9.7	4.1
North Lake[2]	Cornwallis Island	74.77˚N	95.11˚W	29.86	NE	0.6	18.5	5.4
Plateau Lake[3]	Cornwallis Island	74.80˚N	95.19˚W	44.06	NW	0.7*	18*	
Hunting Camp Lake	Bathurst Island	75.75˚N	98.56˚W	26.20	W–SW	4.5	2**	

* Lescord et al. 2015

** Canadian Wildlife Service (2001). However, recent field measurements have recorded slightly greater than 2 m depths in parts of the lake.

Alternate names for lakes used locally: [1]Three Mile Lake; [2]Five Mile Lake; [3]Nine Mile Lake.

TABLE 2. The number, and dates range, of images available for each lake and the number of images removed (unusable) and used in classification (usable). Unusable images exclude images taken during polar darkness (November–February).

Lake	Starting date	Ending date	Total number of images	Unusable number of images	Usable number of images	Usable lake images (%)
Resolute Lake	31/07/2017	31/07/2022	2110	126	743	85.5
Small Lake	22/05/2016	30/07/2022	3910	632	2465	79.6
North Lake	06/08/2019	02/08/2022	6953	513	3566	87.4
Plateau Lake	05/08/2019	03/08/2022	10239	491	3551	87.9
Hunting Camp Lake	25/05/2016	03/08/2022	4518	508	2641	83.9
Total			27730	2270	12966	85.1

FIG. 2. Example set-up of the Reconxy Hyperfire Outdoor camera. Photo: A. Robinson.

control points (GCPs). An additional camera was positioned in front of the installed camera to replicate the view (as not to disrupt the original camera positioning or programming) and capture imagery of the GCPs. Ten rebar pieces, each with bright orange fabric attached for enhanced visibility in the imagery (**Fig. 3**), were placed at known distances from the camera, and their GPS coordinates were recorded using a Garmin eTrex 10 GPS (Accuracy ±10 m, 95% confidence interval). These data supplied coordinates at known points used for scale as reference points during image analysis. This process was repeated at Small Lake on August 7, 2022, and North Lake on August 10, 2022. Logistical constraints prevented the collection of similar GCPs at Plateau Lake and Hunting Camp Lake.

Figure 4 shows the processing flow for each image. During preprocessing, the image quality was assessed manually to determine usability based on visibility and view. Images were considered poor quality if the camera lens was covered by rain or snow, or if the weather was too foggy or hazy to see the lake within the frame. The visibility criteria for selecting photos for classification required at least a partial view of the far side of the lake. Images where the view shifted due to the camera turning in strong wind were still used in most cases. Photos taken during the polar night were excluded.

Georectification, the process of adding geographic information to the image, was completed using Multipoint Geometric Correction, a feature available in ERDAS IMAGINE 2022 (ERDAS). One image from each lake (Resolute Lake, Small Lake, and North Lake) was manually georeferenced by adding the GCPs obtained during field sampling. These reference images were used to acquire spatial information (i.e., surface area of each class; data not included in this manuscript) from the remaining images, as current limitations of the software prevent automation of georectification between raw images. The final product was resampled during geometric transformation using Nearest Neighbour sampling (Parker et al., 1983). Note that georectification is not required for phenology extraction.

A combination of supervised training and unsupervised classification (K-means) produced the best results and usability through the automated classification processes within ERDAS. A total of forty training samples, representing spectral data from the four desired classes (snow, ice, water, shore) covering a mix of weather conditions and transitional ice states, were collected as

FIG. 3. An example of the rebar with flags positioned for the ground truthing survey at North Lake. Image taken by a PC800 HyperFire Professional IR camera.

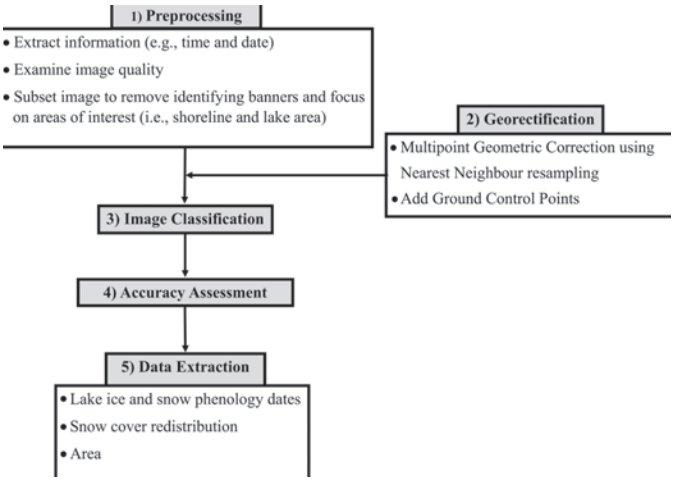

FIG. 4. The analysis process run for camera imagery, repeated for all five lakes except for georectification which was only completed at Resolute Lake, Small Lake and North Lake.

user-defined polygons from ten random images of Resolute Lake and Small Lake. Some images contained multiple classes. These training samples were assumed to be transferable across lakes due to their similar environmental context (i.e., close in latitude, ecological zone) and similar overall ground cover, snow and ice conditions. Signature files, which define the training samples, were created with ten examples for each class from ten different images; these images included varying conditions over the study years, such as sunny, cloudy, and foggy weather, as well as during the transition time for freeze/melt. After creation, the signatures were evaluated using contingency or error matrices, and manual adjustments—such as combining, splitting, or merging training samples—were made to optimize classification performance. The final signature used in the classification was formed by merging several prior mid-processing signatures into one (Step 3, Figure 4), after achieving a sufficient accuracy level based on the error matrices (Hexagon, 2024). The contingency matrix subsequently provides a means to assess how well the training samples align with the anticipated classification (**Table 3**) (Brereton, 2021). This error matrix indicates that the classes match between 85.21% and 98.80%. On average, water was misclassified as ice in 8.17% of samples, while the other classes experienced misclassification rates of less than 5%.

Once the training data were selected, a spatial model was developed to automate the unsupervised classification process within ERDAS, using the K-means method with classes (clusters) defined by the signature files created through the supervised training process (settings are included in Supplementary Table 1). In previous cases, supervised classification outperformed unsupervised classification in land cover classification (Mohd Hasmadi et al., 2009); however, through our methodology development, the best results were achieved using a hybrid classification method.

TABLE 3. Error matrix created from the final signature files based on supervised training data.

Reference Data (%)	Classified Data (%)			
	Snow	Shore	Water	Ice
Snow	96.26	0.04	3.56	2.76
Shore	0.02	98.80	3.06	0.00
Water	0.97	1.14	85.21	2.15
Ice	2.76	0.02	8.17	95.09
Total	100.00	100.00	100.00	100.00

Within the classification model, areas of interest were cropped to include only the lake and shoreline, which varied between the lakes and across different years. The resulting classified images contained categories interpreted as one of the following: shore, water, ice, snow, or unclassified, which referred to pixels not belonging to the other four classes (e.g., sky, banners on images). Some images were excluded due to an Eigenvector classification error in the processing components of ERDAS—specifically, the inability to invert the covariance matrix, indicating that the single-layer image was too homogeneous (n=96)—as well as during post-classification due to poor image quality (n=60). Overall, 85.1% of the usable camera images taken were incorporated into the classification process, leaving only 14.9% of the data set unusable for the analysis (see Table 2).

Following image classification, accuracy assessments were performed in the software to validate the results. 250 stratified random reference points (Congalton, 1991) (independent from training data) were generated for 30 randomly selected images (six images per lake) to calculate classification accuracy, including overall accuracy and a Kappa coefficient, which indicates the improvement of the classification over random chance. 30 images were used to assess classification quality, following Ansari et al. (2017), who also examined freshwater ice using shore-based cameras. In the random selection process, these images were screened to ensure representation of all classes and environmental conditions. We define poor classification as

TABLE 4. Lake ice and snow phenology definitions used in this paper.

Term	Definition
Freeze-up	The transition period between the first appearance of ice on the lake until the lake was completely frozen over.
Snow-on period	The intermittent snow fall period between first snow-on and final snow-on.
First on	The first appearance of ice or snow.
Final on	The date of complete ice or snow cover.
Lake ice/snow cover duration	The number of days between the final ice/snow-on to final ice/snow-off.
Break-up	The transition period between the first appearance of open water until the lake was completely ice-free.
Snow-off period	The time between first snow-off to final snow-off.
First off	The first sign of open water or bare ground.
Final off	The date when the lake was entirely ice-free or the terrain was snow-free for the remainder of the season.

an accuracy below 70%, adequate classification as 70% to 79%, and good classification at 80% or above.

The daily class information from each image was used to extract phenology dates, which were compared with manually identified lake ice and snow phenology dates to assess the accuracy of the automated class detection. Other studies have also validated phenology dates using experienced manual/visual interpretation, a reliable observation method (e.g., Ansari et al., 2017; Han et al., 2020). Root Mean Square Error (RMSE) and Mean Bias Error (MBE) were used to quantify the error between the observed/manually extracted dates and the dates generated by the classification method.

Two dates were identified to describe each freeze-up and break-up period (**Table 4**),

namely the 'first' appearance/disappearance of ice/snow and the 'final' appearance/disappearance, following other cryosphere studies (e.g., Dauginis and Brown, 2021), with appearance/disappearance defined in this study as anywhere in the analysis field of the camera image. The 'first' and 'final' dates do not always differ; for example, the first snow-on and final snow-on dates could be the same for snow phenology if a melt did not occur after the first snow-on.

Areas of ice relative to water and snow cover relative to shore areas were calculated within ERDAS to quantify lake ice and snow coverage, with coverage presented here as percentages for comparison over time.

RESULTS

Image Classification

Accuracy Assessments: Across all lakes and years of sampling, the average classification accuracy was 86%, with a Kappa coefficient (κ) of 0.79. The highest accuracy recorded was 98.8%, with a κ of 0.98 for an image taken at Small Lake in October 2016 (Table S2). This image contained only snow. The classification results perform well when there is only one or two classes in a single image. **Figure 5a** was captured when Resolute Lake was covered in ice and snow, showing the program's ability to distinguish between ice and snow with high accuracy, even under low-light conditions. Figure 5b depicts an image where high classification accuracy and κ are reported, taken during the open water season at Small Lake.

The lowest classification accuracy was 29.6%, with a κ of 0.12 (Supplementary Fig. 1). This image was taken at Small Lake in July 2022 during ice break-up. The conditions were cloudy, with ice and snow visible in the image. Both the highest- and lowest-performing classifications used images from Small Lake. In the particularly poorly classified image, clouds reflected on the lake, which was mainly open water, resulting in a spectral reflectance similar to snow (see Kimes 1983; Nicodemus et al. 1992). Previous studies have also identified errors for classes that spectrally resembled each other (Hung and Treitz, 2020). All images were used throughout the summer (after the ice break-up) to maintain consistency in the landscape and to improve training classes during snow-on/off periods by including examples with the snow-free shore.

Errors during transition periods have been observed by others (Xiao et al., 2018) and were responsible for two poor accuracy assessments in our study lakes (Resolute Lake on June 14, 2018, and Small Lake on June 19, 2018). However, the transition period examples at Hunting Camp Lake showed favourable classifications (classification accuracy ≥ 73.6%, κ ≥ 0.65). Figure 5e provides an example demonstrating the effectiveness of high-quality training samples in distinguishing between ice and snow during break-up. Better visibility and separation between classes at Hunting Camp Lake are likely due to the camera position, as it is situated on an elevated ridge overlooking the lake. However, as discussed in the upcoming assessment sections, this position also led to errors caused by reflections. Although transition periods sometimes had lower accuracy, this was not a consistent pattern across all lakes or transition period images. **Table 5** presents the accuracy assessments for each lake, on average, and indicates that Resolute Lake had the highest classification accuracy, while Small Lake had the lowest. Interestingly, the κ does not follow the same pattern. North Lake (Fig. 5c) and Hunting Camp Lake (Fig. 5e) had equal κ values, and Small Lake had the lowest κ. Camera elevation relative to the shoreline factored into the poor classification results at Small Lake, particularly during transition periods, as the camera is positioned at lake level near the shore, whereas the other lakes have a higher vantage point (Table 1).

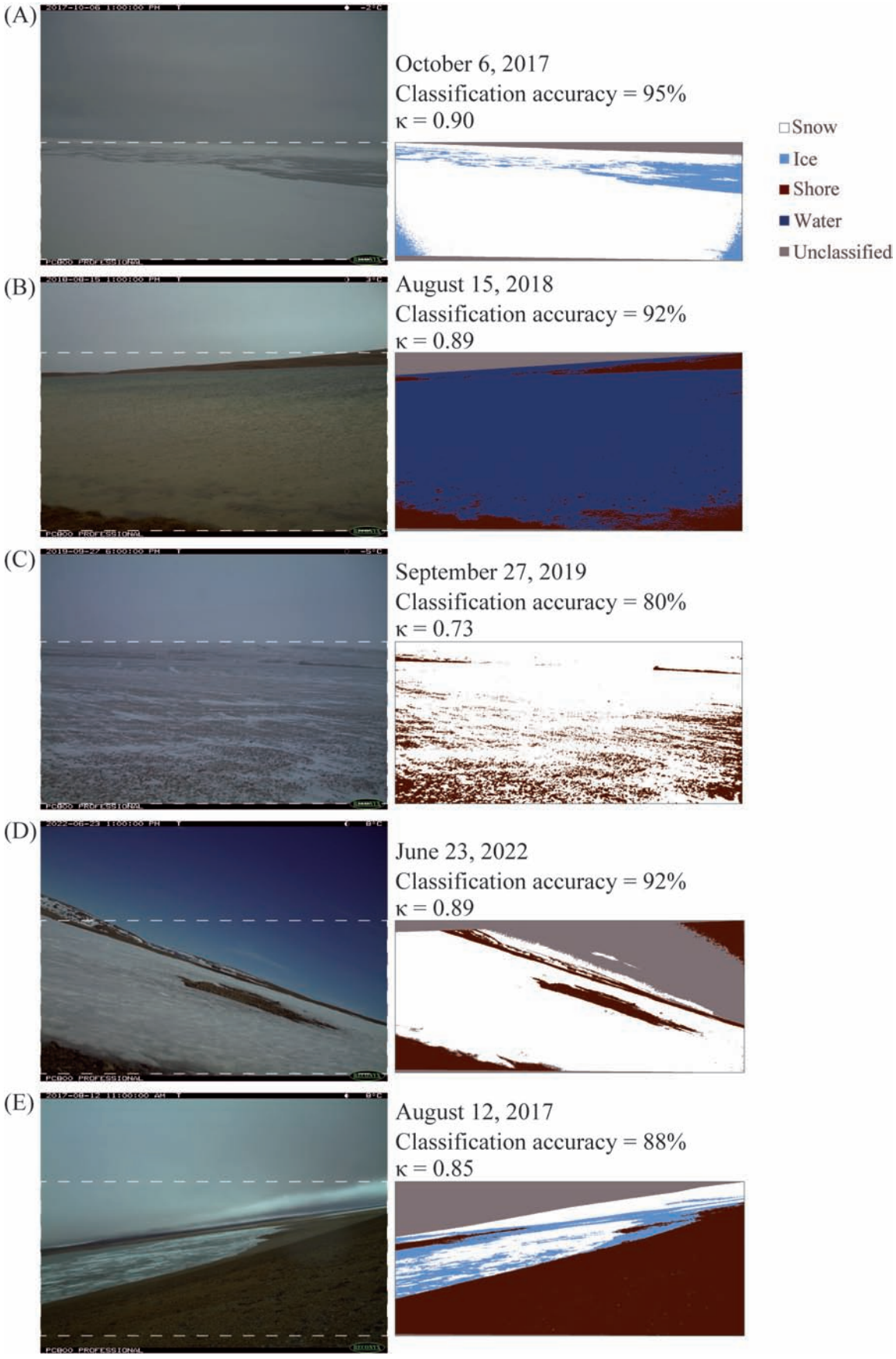

FIG. 5. Examples of digital camera imagery (left) and resulting classified image (right). Classified extent is noted with the dashed white line. Results from (a) Resolute Lake, (b) Small Lake, (c) North Lake, (d) Plateau Lake and (e) Hunting Camp Lake.

TABLE 5. Average accuracy assessment results for each of the five lakes.

Lake	Classification Accuracy (%)	Kappa Coefficient (κ)
Resolute	89.13	0.81
Small	76.16	0.63
North	88.00	0.84
Plateau	87.00	0.83
Hunting camp	87.73	0.84
Average	85.61	0.79

One common factor in misclassification was the presence of cloud cover, which could be misclassified as snow (e.g., Fig. 5e, where the strip of brighter clouds is misclassified as snow) or reflected on the lake›s surface and misclassified as snow. Another source of misclassification occurred with sunny conditions, where sun glare can occur on the lake and is occasionally quantified as snow. Yet, in some cases, cloudy conditions performed better than sunny conditions (as seen on Small Lake on October 16, 2016, for example). Further training samples could be beneficial to reduce this issue, or adjusting the image brightness, depending on the ground conditions; however, this additional labour contradicts the goal of automating the process.

In some cases, local community members and other researchers serviced the cameras by realigning them back to their intended view angle or removing accumulated snow that blocked the lens, which would not have been possible for inaccessible cameras. The ability to classify well, even when the camera view shifted, was valuable. For example, at Plateau Lake, classification results could still track the movement of snow across the landscape, as demonstrated in Figure 5d. The view appeared off-centre with no lake in the frame (June 16, 2022-August 3, 2022) but still provided good visibility of the snow on the shore and the snowmelt period. Additionally, images with low visibility still produced adequate to good classification results. For example, two photos taken during October (transition period) at Resolute Lake had classification accuracies above 93% and κ above 0.90, higher than the average classification accuracy and κ for Resolute Lake (Table S1). In general, the image colour changed when the sun was at its lowest point on the horizon at North Lake and Plateau Lake. Still, the low sun angle did not affect the quality of image classification, as evident in Figure 5c. Thus, similar to Wu et al. (2021), we demonstrate that ground-based cameras are a suitable alternative to mitigate issues associated with the low zenith angle typically encountered with satellite imagery.

Class Distribution and Surface Cover: Quantifying ice and snow in the imagery can provide a valuable understanding of spatial and temporal change in the study area. Seasonal phenology is evident in the imagery at all lakes: periods of snow retreat are visible before snow-free lake ice appears, followed by melt, and then open water and snow-free shorelines become visible (**Fig. 6**). Additionally, the changes in surface cover are evident in snow-covered versus bare ice (**Fig. 7**) and in snow coverage of the lake and its surrounding shoreline (**Fig. 8**) throughout the year. These figures demonstrate detailed information on the ice and snow cover on the lakes with a high temporal resolution. For example, during the freeze-up period in 2017 at Resolute Lake, bare ice was recorded, as shown in Figure 7. In contrast, the ice was entirely snow-covered during formation in 2018. Thus, the snow cover disappearing on ice is evident and detectable based on the classification, which enables the detection and tracking of snow cover retreat and advance on-ice, enhancing the understanding of the phenology of these lakes more than what is possible from space-based imagery.

Manual Extraction vs. Image Classification Results: On average, the first ice-on dates identified by the classification method had an MBE of just 3 days later than the manually extracted dates (**Table 6**), while the final ice-on dates had an MBE of 3 days earlier than the manually extracted dates, indicating that full ice cover was reported slightly before lakes were entirely frozen. For the first ice-off, the classification method had an MBE of only 2 days earlier (noting that the year-to-year fit was quite variable), while for the final ice-off, the classification method had an MBE of 5 days earlier than observed. Combining the ice-on and ice-off timings for all five lakes results in an overall average ice cover duration only 3 days different between the classified and manually extracted dates (308 vs. 311 days).

The first snow-on showed the greatest discrepancy between the two identification methods, with the classification method detecting snow 9 days later (MBE) than the manually observed dates and also having the second-highest RMSE among all snow and ice phenology parameters (**Table 7**). However, the final snow-on date was detected well, only 2 days later (MBE) than the manually extracted dates. The snow-off detection performed well overall but exhibited some variability; overall, the classification method detected the first snow-off 2 days later (MBE) and the final snow-off 1.5 days earlier (MBE). Overall, the snow cover duration was noted as being just two days shorter using the classification method (298 vs. 300 days).

Some differences stem from camera positioning and errors related to sun glare. Despite these issues, the classification results in this work show that using ground-based cameras is a feasible and valuable method for automating ice phenology extraction from a large dataset, while grounded in experienced manual interpretation. The following section provides a more detailed comparison of the phenology dates obtained from each method.

Phenology Comparisons

Lake ice: Freeze-up: Ice-on dates were not synchronized across the lakes, with greater variability between lakes for first ice than for final ice cover (**Fig. 9a** and 9b). The primary factor influencing freeze-up under similar climate conditions is lake morphometry (Brown and Duguay, 2010); shallower lakes tend to freeze earlier under the same climate forcing (Huang et al., 2022). Hunting

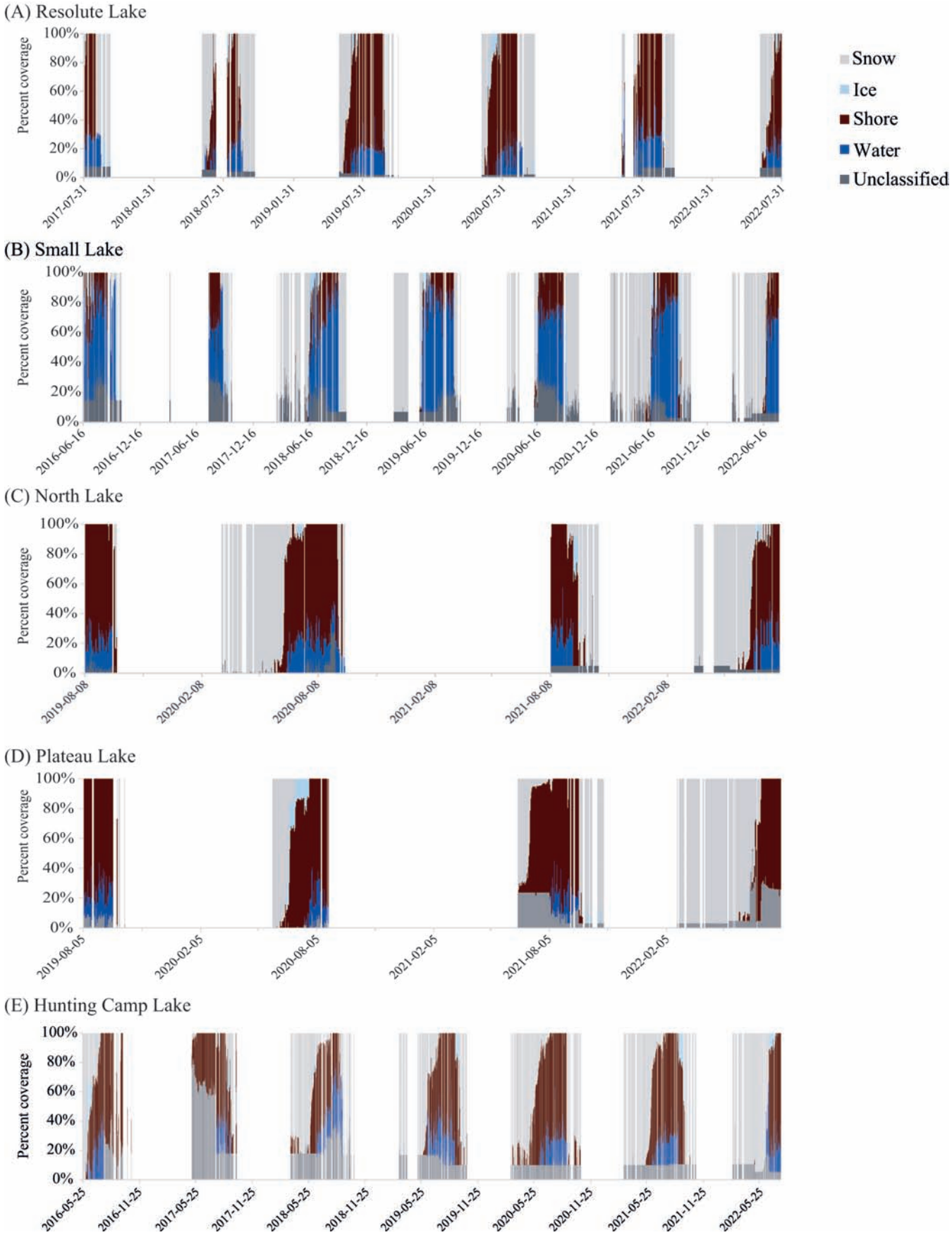

FIG. 6. Percentage coverage of each category for the entire data period from all lakes. The white space represents polar darkness, power interruptions or camera malfunctions. Note different timescales, as not all cameras were set up in the same year.

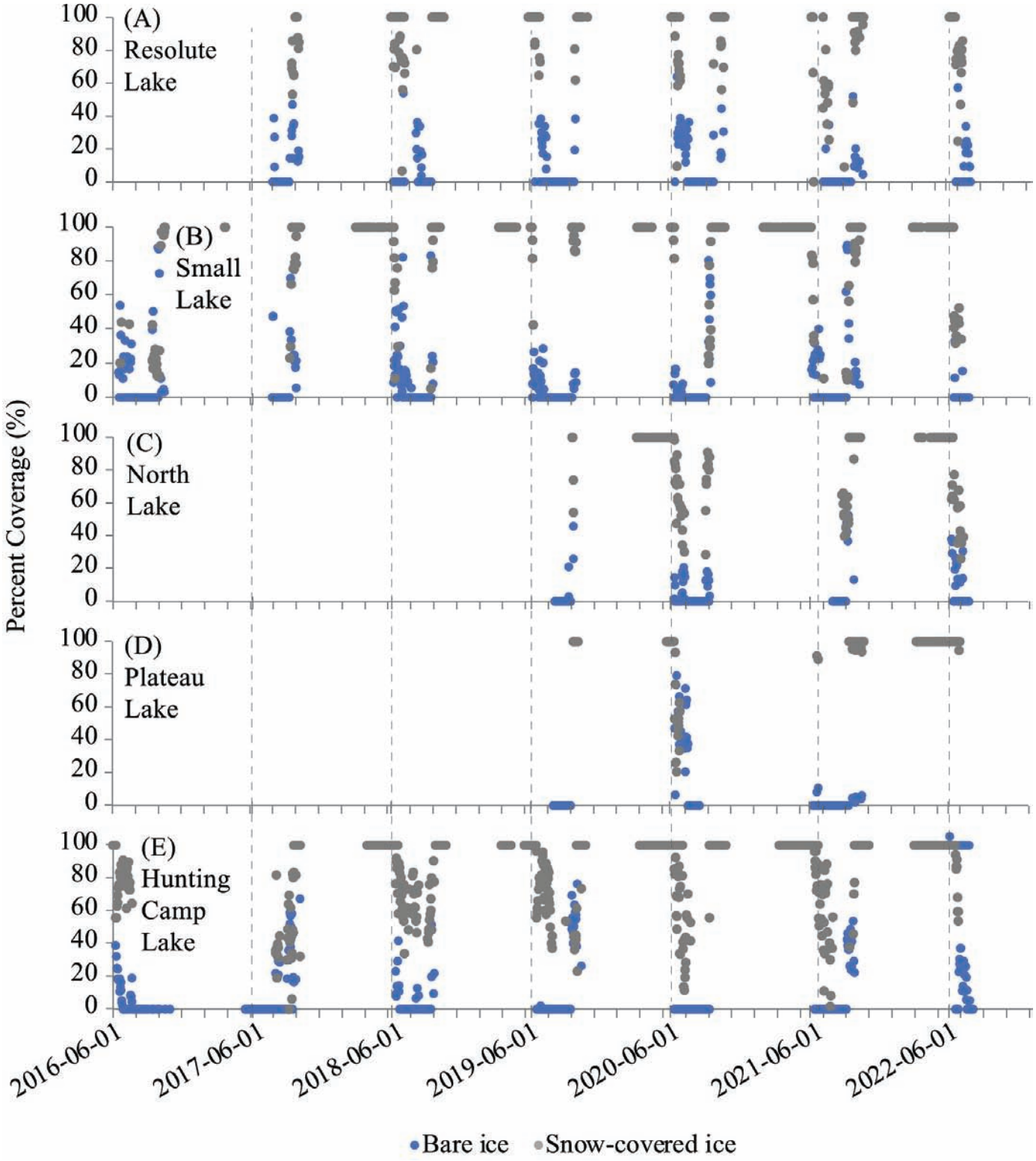

FIG. 7. Lake ice surface cover for the five lakes, for all years with available data based on classification results. Blue circles represent bare ice coverage, and the grey circles represent snow-covered ice. June 1 each year is indicated by a vertical dashed line.

Camp Lake, being shallow (around 2 m deep), can lose heat to the atmosphere more quickly, causing water to cool and freeze faster than in deeper lakes. As shown in Table 6, the mean first ice-on date for all five lakes was September 17, compared to the manually observed average of September 11. The final average ice-on dates ranged from September 14 at Hunting Camp Lake to September 30 at Plateau Lake. This range is slightly broader than the observed range at the same lakes, but the overall inter-lake average differed by only 2 days between the two methods (Table 6).

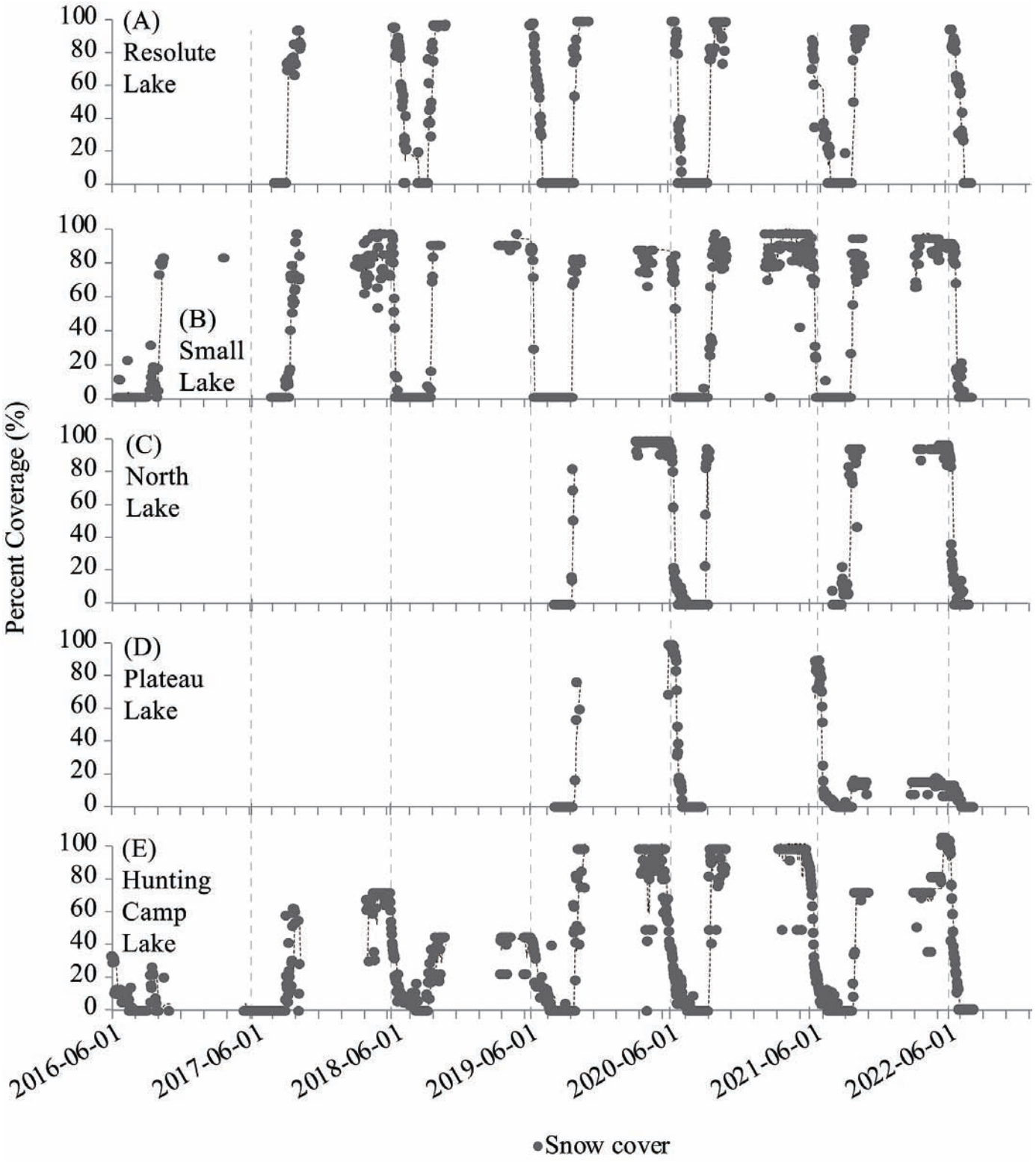

FIG. 8. Snow surface cover for the five lakes for all years with available data based on classification results. Grey circles represent snow coverage; black dotted line represents 5-day moving average to enhance visual clarity of the seasons. June 1 each year is indicated by a vertical dashed line.

The freeze-up period averaged 4 days across all lakes and years, based on the classification dates. In contrast, the manual method yielded a longer freeze, with 11 days for ice freeze-up, due to the earlier detection of ice using the observation method. Hunting Camp Lake had the longest freeze-up rate (close to 30 days in some years) and was influenced by the freeze seasons during 2017, 2018 and 2019, where an incomplete ice cover was present, with one small section of open water persisting into September (**Fig. 10**). Furthermore, the camera was covered by snow for

TABLE 6. Average lake ice phenology dates for all lakes and study years. + only 1 year of data for Plateau. Each year is listed in Tables S3 and S4.

	First Ice-On				Final Ice-On				First Ice-Off				Final Ice-Off			
Lake	Manual	Classified	RMSE	MBE	Manual	Classified	RMSE	MBE	Manual	Classified	RMSE	MBE	Manual	Classified	RMSE	MBE
Resolute	September 16	September 23	6.4		September 25	September 24	2.8		June 29	July 03	8.5		August 06	July 31	6.5	
Small	September 12	September 15	3.5		September 20	September 20	4.7		June 18	June 15	4.1		July 24	July 17	7.2	
North	September 09	September 12	1.4		September 22	September 17	7.3		June 19	June 18	1.4		July 21	July 17	3.6	
Plateau	September 16	September 28	6.1		September 26	September 30	5.0		June 18	June 20	2.0 +		July 27	July 25	2.0 +	
Hunting camp	September 04	September 10	0.6		September 20	September 14	9.8		June 27	July 18	11.9		August 02	July 30	3.3	
All Lakes	September 11	September 17	4.3	2.7	September 22	September 20	6.2	–2.7	June 23	June 22	7.7	–1.7	July 30	July 25	5.6	–4.6

	Average ice cover duration (days)		Average freeze-up season (days)		Average break-up season (days)	
Lake	Manual	Classified	Manual	Classified	Manual	Classified
Resolute	313	310	8	0	36	27
Small	308	301	7	5	37	32
North	303	302	13	5	32	31
Plateau	300	10	0	39	35	
Hunting Camp	317	320	17	6	35	19
All Lakes	311	308	11	4	36	32

TABLE 7. Average snow phenology dates as day-of-year for all lakes and study years. Each year is listed in Tables S5 and S6.

	First Ice-On				Final Ice-On				First Ice-Off				Final Ice-Off			
Lake	Manual	Classified	RMSE	MBE	Manual	Classified	RMSE	MBE	Manual	Classified	RMSE	MBE	Manual	Classified	RMSE	MBE
Resolute	September 04	September 10	6.5		September 14	September 14	0.4		June 09	June 12	2.9		July 15	July 16	5.7	
Small	August 30	September 10	16.5		September 10	September 14	5.4		May 25	May 28	10.3		July 10	June 26	15.6	
North	September 03	September 16	16.9		September 11	September 16	0.6		May 21	May 14	4.5		July 09	July 29	3.0	
Plateau	September 03	September 15	19.8		September 18	September 15	1.0		May 15	May 29	14.0		July 09	July 11	2.0	
Hunting camp	August 25	August 29	7.3		September 10	September 12	1.4		May 18	May 28	7.4		July 07	July 13	18.1	
All Lakes	August 31	September 07	12.2	7.7	September 12	September 14	3.6	1.6	May 25	May 28	7.7	1.8	July 10	July 08	13.0	-1.9

	Average ice cover duration (days)		Average freeze-up season (days)		Average break-up season (days)	
Lake	Manual	Classified	Manual	Classified	Manual	Classified
Resolute	302	305	10	4	37	29
Small	302	281	11	4	46	29
North	300	279	8	0	49	46
Plateau	286	300	15	0	55	43
Hunting camp	300	317	15	14	49	53
All Lakes	300	298	12	6	46	43

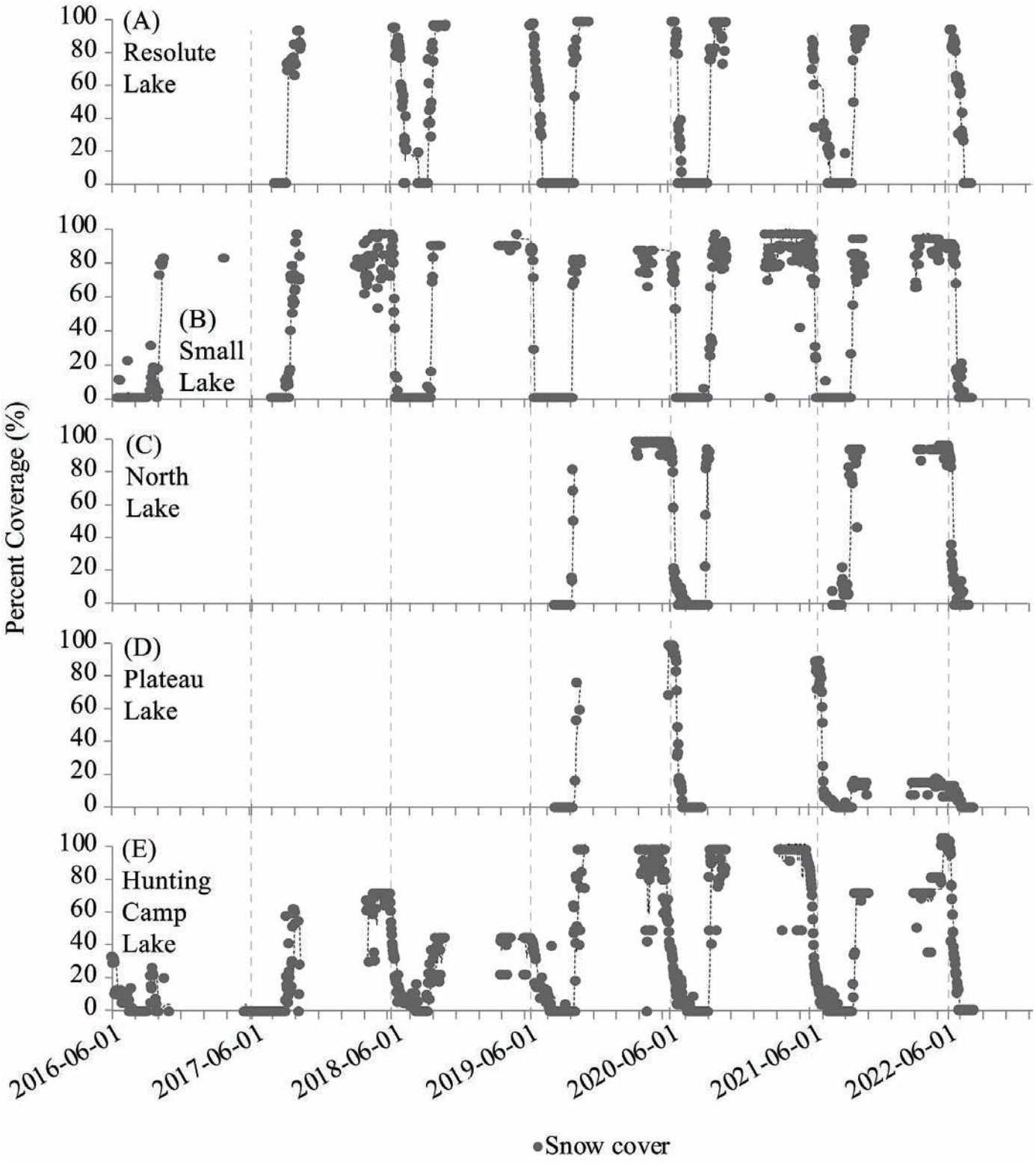

FIG. 9. Classified phenology dates (squares) and manually extracted phenology dates (circles) for all five study lakes for (a) first ice-on dates, (b) final ice-on (c) first ice-off and (d) final ice-off.

several days in 2017 and 2018, and a complete freeze may have occurred while the view was obstructed, resulting in a later recorded date than the actual date.

Lake ice: Break-up: In contrast to ice-on, ice-off was more synchronized between the lakes (Fig. 9c and 9d), as ice melt is primarily influenced by climate (Brown and Duguay, 2010). Across all lakes and years of data, the average first ice-off date was June 22 (June 23, by observation method). The average final ice-off date was July 25, five days earlier than the observation method (Table

FIG. 10. An open patch of water is still visible at Hunting Camp Lake, contributing to a longer freeze-up period and later final ice-on.

6). Small and North Lakes had the earliest average final ice-off dates on July 17 (compared to July 24 for Small and July 21 for North using the observation method) (Table 6), while Resolute Lake had the latest on July 31 (versus August 6 by observation method).

The average final ice-off date for Small Lake is similar to the single date of July 22, 1981, reported in a previous study, when the lake was ice-free (Heron and Woo, 1994). At Hunting Camp Lake, the average first ice-off was identified as 18 June, but was observed manually from the imagery to be over a week later, on June 27 (RMSE 12 days). At this lake in particular, the sun glare on the water or floating ice pan makes identifying the first ice-off difficult by observation, although classification accuracy was 87.7%, indicating good overall accuracy. This likely caused the discrepancy, as other lakes had first ice-off dates within four days of each other between methods. The average date for the appearance of open water on Hunting Camp Lake, as detected via satellite imagery from 1997 to 2011, was 25 June (Surdu et al. 2016). The mean final ice-off date from 1997 to 2011 was 26 July, close to recent years when the ice was fully gone by 30 July (classification method) or 2 August (observation method). The later dates result from the improved spatial resolution of the cameras, which enables the detection of smaller remaining ice regions than those detected by satellites used in the comparable study, which had a finest resolution of 30 m (Surdu et al., 2016). These ice-off dates are also similar to those of other lakes, such as West Lake and East Lake on Melville Island, where ice-off usually occurs in mid-July to early August (Dugan et al. 2012).

Compared to freeze-up, there was more variability in the break-up duration, with standard deviations of 11 and 9 days, than in the freeze rates, with standard deviations of 6 and 8 days (classified and observed, respectively) (Supplemental Tables 3, 4). This difference is likely caused by the floating ice pans, which vary from year to year depending on melt rates and wind patterns during the break-up period.

Ice cover break-up duration lasted an average of 32 days (22 June–25 July) using the classification method, but 4 days longer with the observed method – of note, though, three additional years' first ice off dates were possible with the observed method, so some variation is expected. The classification method had difficulties with the 2018 ice-off season at Hunting Camp Lake, identifying the first ice-off date as June 12, whereas observation indicated 28 June. The wet-looking, snow-free ice appeared bright blue this day from reflections and was misclassified as water, leading to a skewed break-up duration of 60 days when it was 46 days from observation. This year was also particularly challenging to visually identify the beginning of break-up due to reflections on the ice near shore that made it difficult to distinguish water-on-ice from open water. Hunting Camp Lake had a slightly longer break-up duration than previously reported (29 days from melt onset to water clear of ice, Surdu et al. 2016), which is not unexpected, as our cameras can resolve more detail than the satellites used in that study.

Snow: Snow-on: For the landscape surrounding all five lakes, the average first snow-on date was 7 September, according to the classification method, and August 31, based on the observation method. This parameter exhibited the second-highest RMSE and the largest MBE among all the phenology parameters (Table 7) (**Fig. 11a**, b). Final snow-on, however, was accurately detected using the classification method, with an average difference of only 2 days from observations, and the snow-on duration averaged 6 days (or 12 days when using the observation method) (Table 7).

Hunting Camp Lake experienced the earliest average snow-on date, on 29 August (25 August, by observation method), which occurs about six weeks after the snow melted from the previous season. The overall temperature and precipitation conditions at Nanuit Itillinga are similar to those at Resolute (Young and Brown, 2023), but some differences in snowfall timing and duration are expected, as Hunting Camp Lake is approximately 140 km from the other lakes.

While the small variability in average dates between the Cornwallis Island lakes in relatively close proximity can be explained by local precipitation variability, along with camera direction and local topography, the differences between the classification and observation methods highlight some challenges with detecting snow-on. These lakes showed an average snow-on of 10 days later using the classification method (12 September versus 2 September). The first and final snow-on timing is often the same using the classification method, whereas visually, in some years, a very small snowfall may be visible but is not recognized by the classification method. For example, Plateau Lake in Fall 2019: a light snowfall occurred on 30 August, leaving a small amount of snow in a topographic depression that quickly melted by the next day. The camera view was obscured (by snow/ice on the lens) from September 21 – 26, but manual inspection reveals that you can see through the haze on September 26 and see snow on the ground, but

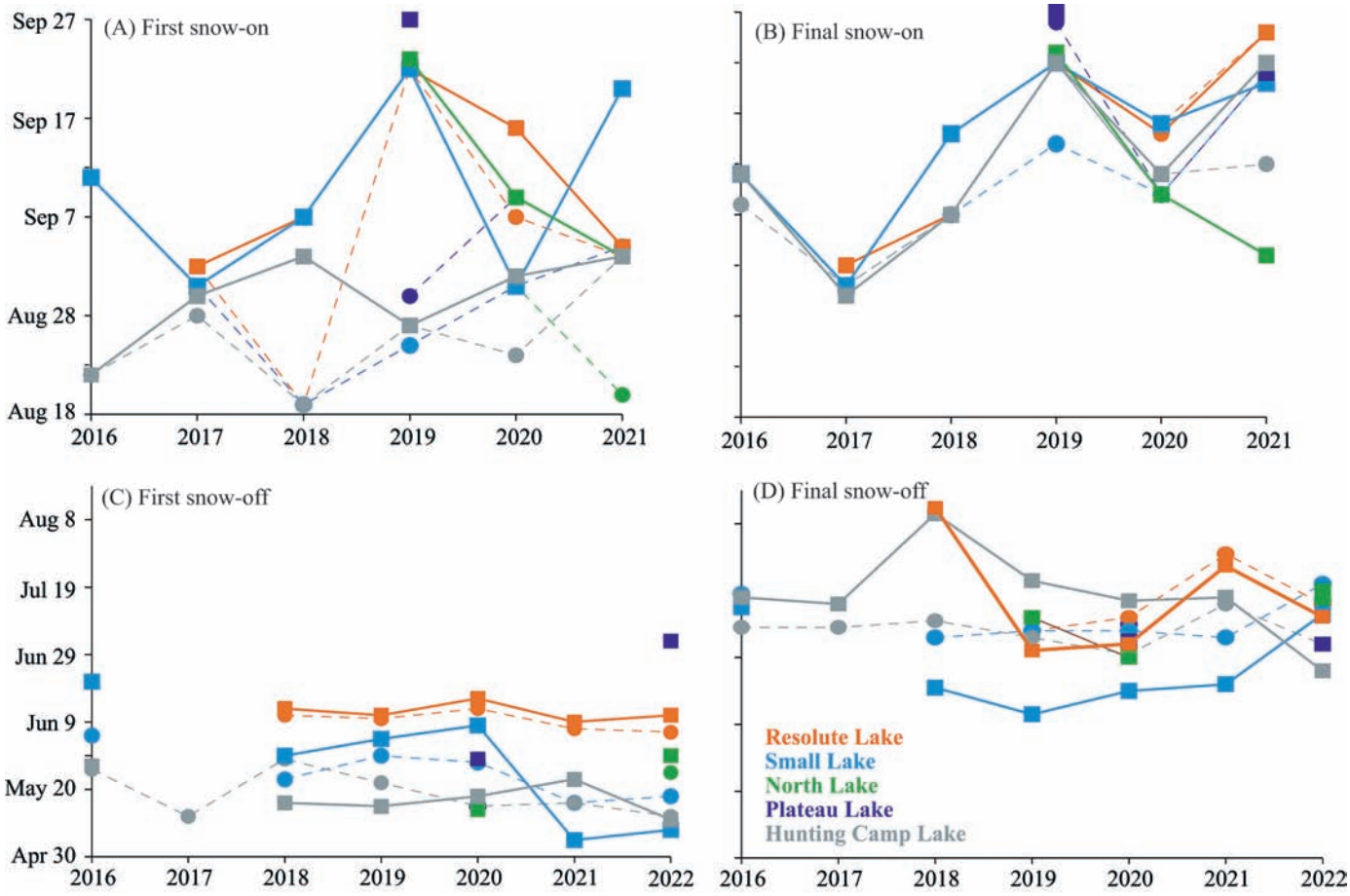

FIG. 11. Classified phenology dates (squares) and manually extracted phenology dates (circles) for all five study lakes for (a) first snow-on dates, (b) final snow-on (c) first snow-off and (d) final snow-off.

the image is not clear until September 27 (the date detected using the classification method). Overall, as highlighted in Figure 11a and b, there is better coherence between the methods and the study lakes for detecting the final snow-on than the first snow-on.

Snow: Snow-off: Overall, both methods extracted comparable average days for first and final snow-off (differing by 3 days for the first snow-off and 2 days for the final snow-off), yet while the MBE was small, the RMSE was highest among all variables for snow-off, primarily due to errors related to Small Lake and Hunting Camp Lake caused by camera positioning, as discussed below.

The average first snow-off date was 28 May (25 May, by observation method). Resolute Lake experienced the latest first snow-off with both methods (Fig. 11), while the earliest date varied between methods (North Lake by classification method and Plateau by observation method). At Hunting Camp Lake, the average first snow-off date was 28 May (18 May, by observation method), which is nearly a month earlier than a previous satellite-based study conducted at Polar Bear Pass (now Nanuit Itillinga) (using QuikSCAT, ~ 2.25 km resolution), which recorded 11 June as the start of snow-off from 2000–09 (Howell et al. 2012), demonstrating the enhanced ability for local-scale detection using ground-based imagery.

The average final snow-off date was 8 July, which is 2 days earlier than the date determined through observations. The earliest final snow-off with the classification method was Small Lake (26 June), while the earliest with visual inspection was Hunting Camp Lake (7 July). Once again, at Hunting Camp Lake, the improved resolution led to differences from the space-based final snow-off timing (Howell et al. 2012), with a difference of approximately a week using the ground-based data. Using ground-based manual observation dates for Hunting Camp Lake, snow offset lasted an average of 49 days from 2016 to 2022. In contrast, using space-based methods (for an earlier set of years) detected a 17-day offset period. This is an example of how ground-based imagery improves the ability to detect local land cover changes, such as bare patches of ground in late May and persistent patches of snow toward the end of the melt season.

The final snow-off dates extracted through the classification method at Small Lake were heavily influenced by camera position and movement. The camera was placed very close to the shore, resulting in only a small shoreline segment where snow could be detected. During some years of melting, water levels rose above this shoreline segment. Additionally, the camera's position shifted slightly over the season, impacting the masked regions. The hills behind

the lake contain small, late-lying snowbeds in topographic depressions, which are masked out in the classification method, leading to discrepancies between automated and visual detection. Using manual dates that only represent the small shoreline strip in the imagery aligns with the classification method for snow-off detection.

The large difference between classified and manually extracted dates at Hunting Camp Lake is due to sun glare. The floating ice pan in 2018 and 2020 reflected very brightly the day before the final snow-off, suggesting pixel values more indicative of snow. For comparison, removing the incorrect classifications from the calculations restores the RMSE at Small and Hunting Camp to align with the other lakes, around 5-6 days.

For all the lakes, the average snow retreat period was similar, with only a 3-day difference when using the classification method compared to the observation method.

Snow: Snow Cover Redistribution: The camera imagery revealed the variability in snow conditions on the study lakes. For example, the snow decreasing around the Resolute Lake camera was visible through May 2022, despite many days when views were obstructed by snow at the height of the camera; when clear views were possible, the reduction in snow on the landscape was apparent (**Fig. 12a**). At Small Lake, the imagery showed how conditions changed over the season, with patchy areas of ice visible in some parts and, at other times, snow that appeared compact and windblown, with sparse snow cover on the lake. (Fig. 12b, 12c). Combining the imagery with Figure 7 can provide a detailed explanation of snow cover redistribution throughout the season, which has implications for lake ice thickness below (e.g., Brown and Dugay, 2010).

Overall Duration and Relationships Between Ice and Snow: Despite the variation in ice detection between methods, the average ice cover duration for all lakes combined was 308 days using the classification methods, and only 3 days later at 311 days using observations (Table 6), consistent with studies noting that ice duration can last over ten months. (Heron and Woo, 1994). The overall average SCD was just 2 days shorter using the classification method (298 days) than the observed method (300 days).

Some current studies have shown a decrease in SCD with later snow onset and earlier snow offset in spring across the pan-Arctic (e.g., Liston and Hiemstra 2011, Brown et al. 2021). Future predictions indicate a decrease in snow cover in Canada, especially during the spring months of April, May, and June (Mudryk et al. 2018). However, studies focusing on recent years (1997–2019) for the Canadian High Arctic (rather than the pan-Arctic) have shown that SCD changes were not statistically significant within the short time frame examined, although the timing shifted earlier, with earlier snow onset and melt (Dauginis and Brown, 2020; Dauginis and Brown, 2021). A lengthening of SCD occurred from 2006–2013 in Nanuit Itillinga (Young et al. 2018), with earlier snow-on timing (though not statistically significant) and no change in snow-off noted when the record was extended through 2021 (Young and Brown 2023). This discrepancy from other trends may be due to the short study period, as the long-term 40-year record from Resolute indicates both earlier snow-off and later snow-on (Young and Brown, 2023). Therefore, the subtle differences between study sites and time periods highlight the need for continuous Arctic monitoring, especially at the local scale, to track and understand emerging trends.

While the ice melt period and the snow retreat period differed in duration by approximately 1.5 weeks, the snow retreat period began three weeks earlier (at the end of May), whereas ice began to visibly retreat in late June. Similarly, the lake ice duration and SCD were also approximately 1.5 weeks different, at 308 days and 298 days, respectively. On average, snow cover was present for the season for about 1.5 weeks before the ice formed a full cover, and it was fully gone from the landscape about 3 weeks before the ice cover was completely clear from the lakes (Table 6 and Table 7). Considering these two cryosphere elements in tandem is essential, as snow acts as an insulator, inhibiting ice growth, while also delaying ice decay through its higher albedo when present on the ice (Brown and Duguay, 2010; Serreze and Barry, 2014; Robinson et al., 2021).

DISCUSSION AND CONCLUSION

In this study, we present a novel and accessible, semi-automated method for using remote sensing tools in conjunction with ground-based cameras, along with a straightforward and user-friendly methodology for monitoring and quantifying snow and lake ice, which is crucial in a changing Arctic environment. For nearly 13,000 images across five locations and several years, the overall classification accuracy was 85.9%, with a Kappa coefficient of 0.79. The methods presented can be applied to other disciplines that are related to tracking land cover changes, including glaciology and hydrology. Being able to quantify and track land cover changes throughout the year is particularly useful for ecological and biological studies. For example, shorebird breeding is closely tied to the timing when snow cover on the ground reaches the 50% point in the spring (Smith et al., 2010; Anderson et al., 2023), and the breeding season will be affected by changing snow cover conditions.

Lake ice and snow phenology dates determined from the classified camera imagery and validated based on experienced manual observations of the imagery aligned well, within 2 to 5 days for the ice phenology and 2 to 9 days for snow phenology. In general, aside from the noted classification errors discussed previously, first ice-on tended to be slightly earlier from visual inspection than using the classified method, for example, due to the ability to visual distinguish a thin skim of ice from subtle differences in smoothness – these would not be much different in terms of pixel reflectance in the imagery. The final ice-on was the opposite, as we can see small areas with no ice that

FIG. 12. (a) Resolute Lake from the digital camera imagery on May 13, 2022. The snow depth is just below the lens of the camera; (b) The view from Small Lake on October 24, 2021 and (c) 10 May 10 2022 (right). Snow redistribution is visible in the digital camera imagery over a phenological year.

are later than the classification can detect. The first ice-off dates were the most similar between the methods, but still presented challenges, as the subtle changes nearshore at the beginning of breakup can be difficult to distinguish. The final ice-off was a little later visually, but similar to the ice-on situation, with ice that can be visually distinguished. The differences in snow dates are similar to those in ice, in that visually, we can detect small patches or thin scattering of snow cover, leading to, for example, larger discrepancies in the snow-on timing.

Another aspect to consider is the subjectivity of visual analysis used for validating the classification method. We recommend at least two people assess the imagery when using manual extraction techniques to reduce subjectivity errors. Visual observation of snow and ice phenology by researchers is common (e.g., Ansari et al., 2017; Han et al., 2020), and the goal of this research was to develop an automated method to handle a large volume of data while retaining expert ground-based interpretation of the imagery. Despite the small differences in the dates obtained through each technique, the overall durations were quite similar. This study demonstrated the utility of ground-based imagery, as finer resolution captures small changes, such as snow-free ground in May, that are not detectable from most satellite-based platforms. Furthermore, this blend of remote sensing and ground-based data could be very beneficial for obtaining finer-resolution data than is attainable from space, or for validating space-based or modelling work, which is extremely challenging in remote Arctic locations (e.g., Murfitt et al., 2018; Robinson and Brown, 2025).

Some of the years where the classification method had larger differences with the manually observed dates can be attributed to camera placement and can be alleviated in future studies. For example, at Small Lake, the camera was too close to the shoreline, which posed difficulties during the melt when the water level changed, overflowing the shoreline. This camera has since been relocated to a higher position on the surrounding hill. The challenges with the cameras tipping/rotating during the season (e.g., Plateau Lake) have since been reduced; the current setup of the cameras uses a T-bar rather than rebar, allowing for a flat surface on which the camera can be more securely mounted.

Future research can explore several possibilities to improve classification. Transition periods remain an area for improvement in classification results (e.g., thin skim ice in the fall, or wet melting ice in the spring). Reducing cloud-related misclassification errors is possible through more refined image masking to eliminate the sky from the analysis; with the improved camera stability, this will be possible in future work. Our overall methods are not program-specific and can be recreated with other software to further enhance their effectiveness and increase efficiency through additional automation. Although this analysis was conducted in ERDAS Imagine, other image classification software could be used to recreate the workflow, with or without the georectification step included (e.g., open-source QGIS, ArcPro, etc., or even adapted for direct coding software such as Python). Further automation may also be possible for future work through a temporal consistency check to flag or remove misclassifications that would more than likely be due to errors, for example, open water detected during a typically ice-covered period, though thorough knowledge of the region's climate and the seasonal variability experienced would be required. To further build on this work, the addition of a snow stake to monitor snow depth changes within the camera view would be extremely beneficial. The snow stake would serve as a ground-truthing tool and enable measuring snow accumulation; however, this was not possible for this study, as the stakes would pose a safety hazard to snowmobilers in the area. For future deployments, optimal camera setups would keep the camera orientation offset from the seasonal sun azimuth, use elevated ridges or higher positions, where possible, and maintain consistent geometry across years to support comparison. Additionally, care should be taken to ensure the camera is securely mounted to the mounting post; we now use bolts through T-bar in most cases, but if cold weather zip ties are being used, consider adding a mounting strap (e.g., those that come with trail cameras intended to be used on trees) as well to help reduce camera movement in extreme weather. While logistics can limit the number of cameras around a lake, having more than one camera per lake (or a network of cameras surrounding a lake), or using any topographic advantages possible to position the cameras for lake-wide views, could provide an even more in-depth comparison of spatial variability and subpixel analysis for satellite-based work. Arctic research presents numerous logistical challenges; however, monitoring changes in lake ice and snow will become an increasingly important priority in a rapidly warming Arctic environment. Ground-based automated cameras alleviate some of these monitoring restraints and provide incredibly valuable insight into spatial conditions in such remote locations, as well as add confidence to space-based or modelling-based phenology work. These methods could also be adapted to maintain near-real time updates on ice road conditions using shoreline cameras (where cellular or satellite capabilities permit), which could be crucial for economic resilience and security in Canada and other countries in the Northern Hemisphere where snow and ice play a crucial role in the environment.

ACKNOWLEDGEMENTS

This project was funded by an NSERC Discovery Grant and the Northern Scientific Training Program, with logistical support through the Polar Continental Shelf Program. We would like to thank Debbie Iqaluk, Noah Bacal, Daniel Serrano-Cadena, and Xiaomeng Zuo for field assistance, and Alex Cabaj for suggestions to strengthen an early draft of this manuscript.

During the preparation of this work, the authors used the software Grammarly in order to assist with proofreading for grammatical errors and typos in the manuscript. After using this tool, the author(s) reviewed and edited the content as needed and take full responsibility for the content of the publication.

REFERENCES

Anderson, C.M., Fahrig, L., Rausch, J., Martin, J.-L., Daufresne, T., and Smith, P.A., 2023. Climate-related range shifts in Arcti-breeding shorebirds. Ecology and Evolution 13(2): e9797. https://doi.org/10.1002/ece3.9797

Ansari, S., Rennie, C.D., Seidou, O., Malenchak, J., and Zare, S.G. 2017. Automated monitoring of river ice processes using shore-based imagery. Cold Region Science and Technology 142:1–16. https://doi.org/10.1016/j.coldregions.2017.06.011

Ariano, S.S., and Brown, L.C. 2019. Ice processes on medium-sized north-temperate lakes. Hydrological Processes 33(18):2434–2448. https://doi.org/10.1002/hyp.13481

Arp, C.D., Jones, B.M., Whitman, M., Larsen, A., and Urban, F.E. 2010. Lake temperature and ice cover regimes in the Alaskan subarctic and Arctic: Integrated monitoring, remote sensing, and modeling. Journal of the American Water Resources Association 46(4):777–791. https://doi.org/10.1111/j.1752-1688.2010.00451.x

Atkinson, D.M., and Treitz, P. 2012. Arctic ecological classifications derived from vegetation community and satellite spectral data. Remote Sensing 4(12):3948–3971. https://doi.org/10.3390/rs4123948

Benson, B.J., Magnuson, J.J., Jensen, O.P., Card, V.M., Hodgkins, G., Korhonen, J., Livingstone, D.M., et al. 2012. Extreme events, trends, and variability in Northern Hemisphere lake-ice phenology (1855–2005). Climate Change 112(2): 299–323. https://doi.org/10.1007/s10584-011-0212-8

Bokhorst, S., Pedersen, S.H., Brucker, L., Anisimov, O., Bjerke, J.W., Brown R.D., Ehrich, D., et al. 2016. Changing Arctic snow cover: A review of recent developments and assessment of future needs for observations, modelling, and impacts. Ambio 45(5):516–537. https://doi.org/10.1007/s13280-016-0770-0

Bothmann, L., Menzel, A., Menze, B.H., Schunk, C., and Kauermann, G. 2017. Automated processing of webcam images for phenological classification. PLoS One 12(2): 0171918. https://doi.org/10.1371/journal.pone.0171918

Brereton, R.G. 2021. Contingency tables, confusion matrices, classifiers and quality of prediction. Journal of Chemometrics 35(11): e3331. https://doi.org/10.1002/cem.3331

Brown, L.C., and Duguay, C.R. 2010. The response and role of ice cover in lake-climate interactions. Progress in Physical Geography: Earth and Environment 34(5):671–704. https://doi.org/10.1177/0309133310375653

Brown, R.D., Smith, C., Derksen, C., and Mudryk, L. 2021. Canadian in situ snow cover trends for 1955–2017 including an assessment of the impact of automation. Atmosphere – Ocean, 59(2):77–92. https://doi.org/10.1080/07055900.2021.1911781

Canadian Wildlife Service. 2001. Information sheet on Ramsar Wetlands. Accessed 30 November 2022. https://rsis.ramsar.org/RISapp/files/RISrep/CA245RIS.pdf

Chasmer, L., Hopkinson, C., Veness, T., Quinton, W., and Baltzer, J. 2014. A decision-tree classification for low-lying complex land cover types within the zone of discontinuous permafrost. Remote Sensing of Environment 143:73–84. https://doi.org/10.1016/j.rse.2013.12.016

Congalton. R.G. 1991. A review of assessing the accuracy of classifications of remotely sensed data. Remote Sensing of Environment 37(1):35–46. https://doi.org/10.1016/0034-4257(91)90048-B

Dauginis, A.L.A., and Brown, L.C. 2020. Sea ice and snow phenology in the Canadian Arctic Archipelago from 1997 to 2018. Arctic Science 7(1):182–207. https://doi.org/10.1139/as-2020-0024

Dauginis, A.A., and Brown, L. 2021. Recent changes in pan-Arctic sea ice, lake ice, and snow on/off timing. The Cryosphere 15:4781–4805. https://doi.org/10.5194/tc-2021-52

Du, J., Kimball, J.S., Duguay, C., Kim, Y., and Watts, J.D. 2017. Satellite microwave assessment of Northern Hemisphere lake ice phenology from 2002 to 2015. The Cryosphere 11(1):47–63. https://doi.org/10.5194/tc-11-47-2017

Dugan, H.A., Lamoureux, S.F., Lewis, T., and Lafrenière, M.J. 2012. The impact of permafrost disturbances and sediment loading on the limnological characteristics of two high Arctic lakes. Permafrost and Periglacial Processes 23(2):119–126. https://doi.org/10.1002/ppp.1735

Enderle, D.I., and Weih, R.C., Jr. 2005. Integrating supervised and unsupervised classification methods to develop a more accurate land cover classification. Journal of the Arkansas Academic Sciences 59: 10. https://scholarworks.uark.edu/jaas/vol59/iss1/10/

Environment and Climate Change Canada (ECCC). 2022. Weather, climate and hazard: Historical climate data. Accessed 6 December 2021. https://climate.weather.gc.ca/index_e.html

French, H., and Slaymaker, O. 2011. Changing cold environments: A Canadian perspective. New Jersey: Wiley-Blackwell.

Geldsetzer, T., van der Sanden, J., and Brisco, B. 2010. Monitoring lake ice during spring melt using RADARSAT-2 SAR. Canadian Journal of Remote Sensing 36(2):S391–S400. https://doi.org/10.5589/m11-001

Hampton, S.E., Galloway, A.W.E., Powers, S.M., Ozersky, T., Woo, K.H., Batt, R.D., Labou, S.G., et al. 2017. Ecology under lake ice. Ecology Letters 20(1): 98–111. https://doi.org/10.1111/ele.12699

Han, W., Huang, C., Duan, H., Gu, J., and Hou, J. 2020. Lake phenology of freeze-thaw cycles using random forest: A case study of Qinghai Lake. Remote Sensing 12(24): 4098. https://doi.org/10.3390/rs12244098

Heron, R., and Woo, M.-K. 1994. Decay of a high Arctic lake-ice cover: Observations and modelling. Journal of Glaciology 40(135):283–292. https://doi.org/10.1017/S0022143000007371

Hexagon, 2024. ERDAS documentation, Field Producers Guide. Accessed March 2026. https://hexagongeospatial.fluidtopics.net/r/uOKHREQkd_XR9iPo9Y_Ijw/khBQoaH4ne8R6PVMWZ7Ubw.

Howell, S.E.L., Assini, J., Young, K.L., Abnizova, A., and Derksen, C. 2012. Snowmelt variability in Polar Bear Pass, Nunavut, Canada, from QuikSCAT: 2000–2009. Hydrological Processes 26(23):3477–3488. https://doi.org/10.1002/hyp.8365

Huang, L., Timmermann, A., Lee. S.-S., Rodgers, K.B., Yamaguchi, R., and Chung, E.-S. 2022. Emerging unprecedented lake ice loss in climate change projections. Nature Communications 13: 5798. https://doi.org/10.1038/s41467-022-33495-3

Hung, J.K.Y., and Treitz, P. 2020. Environmental land-cover classification for integrated watershed studies: Cape Bounty, Melville Island, Nunavut. Arctic Science 6(4):404–422. https://doi.org/10.1139/as-2019-0029

Kimes, D.S. 1983. Dynamics of directional reflectance factor distributions for vegetation canopies. Applied Optics 22(9):1364–1372. https://doi.org/10.1364/AO.22.001364

Latifovic, R., and Pouliot, D. 2007. Analysis of climate change impacts on lake ice phenology in Canada using the historical satellite data record. Remote Sensing of Environment 106(4):492–507. https://doi.org/10.1016/j.rse.2006.09.015

Lenormand, F., Duguay, C.R., and Gauthier, R. 2002. Development of a historical ice database for the study of climate change in Canada. Hydrological Processes 16(18):3707–3722. https://doi.org/10.1002/hyp.1235

Lescord, G.L., Kidd, K.A., Kirk, J.L., O'Driscoll, N.J., Wang, X., and Muir. D.C.G. 2015. Factors affecting biotic mercury concentrations and biomagnification through lake food webs in the Canadian high Arctic. Science of the Total Environment 509-510:195–205. https://doi.org/10.1016/j.scitotenv.2014.04.133

Leshkevich, G., and Nghiem, S.V. 2013. Great Lakes ice classification using satellite C-band SAR multi-polarization data. Journal of Great Lakes Research 39(S1):55–64. https://doi.org/10.1016/j.jglr.2013.05.003

Liston, G.E., and Hiemstra, C.A. 2011. The changing cryosphere: Pan-Arctic snow trends (1979–2009). Journal of Climate 24(21):5671–5712. https://doi.org/10.1175/JCLI-D-11-00081.1

MacKay, M.D., Verseghy, D.L., Fortin, V., and Rennie, M.D. 2017. Wintertime simulations of a boreal lake with the Canadian Small Lake Model. Journal of Hydrometeorology 18(8):2143–2160. https://doi.org/10.1175/JHM-D-16-0268.1

McCrystall, M., Stroeve, J., Serreze, M., Forbes, B., and Screen, J. 2021. New climate models reveal faster and larger increases in Arctic precipitation than previously projected. Nature Communications 12: 6765. https://doi.org/10.1038/s41467-021-27031-y

Mohd Hasmadi, I., Pakhriazad, H.Z., and Shahrin, M.F. 2009. Evaluating supervised and unsupervised techniques for land cover mapping using remote sensing data. Malaysian Journal of Society and Space 5(1):1–10. https://www.proquest.com/openview/3ce55d3fe96fef40bc5d5167ff0f18f2/1?pq-origsite=gscholar&cbl=4916363

Mudryk, L.R., Derksen, C., Howell, S., Laliberté, F., Thackeray, C., Sospedra-Alfonso, R., Vionnet, V., Kushner, P.J., and Brown, R. 2018. Canadian snow and sea ice: Historical trends and projections. The Cryosphere 12(4):1157–1176. https://doi.org/10.5194/tc-12-1157-2018

Mudryk, L., Santolaria-Otín, M., Krinner, G., Ménégoz, M., Derksen, C., Brutel-Vuilmet, C., Brady, M., and Essery, R. 2020. Historical Northern Hemisphere snow cover trends and projected changes in the CMIP6 multi-model ensemble. The Cryosphere 14(7):2495–2514. https://doi.org/10.5194/tc-14-2495-2020

Mudryk, L., Elias Chereque, A., Derksen, C., Luojus, K., and Decharme B. 2022. Terrestrial snow cover. NOAA Technical Report OAR ARC 22-03, Arctic report card 2022. https://doi.org/10.25923/yxs5-6c72

Murfitt, J., and Duguay, C.R. 2021. 50 years of lake ice research from active microwave remote sensing: Progress and prospects. Remote Sensing of Environment 264: 112616. https://doi.org/10.1016/j.rse.2021.112616

Murfitt, J., Brown, L.C., and Howel, S.E.L. 2018. Evaluating RADARSAT-2 for the Automated Monitoring of Lake Ice Phenology Events in Mid-Latitudes Remote Sensing 10(10):1641. https://doi.org/10.3390/rs10101641

Nicodemus, F., Richmond, J., Hsia, J., Ginsberg, I., and Limperis, T. 1977. Geometrical considerations and nomenclature for reflectance. Ann Arbor: US Department of Commerce, National Bureau of Standards. https://nvlpubs.nist.gov/nistpubs/Legacy/MONO/nbsmonograph160.pdf

Parker, J.A., Kenyon, R.V., and Troxel, DE. 1983. Comparison of interpolating methods for image resampling. IEEE Transactions on Medical Imaging 2(1):31–39. https://doi.org/10.1109/TMI.1983.4307610

Prowse, T., Knut, A., Beltaos, S., Bonsal, B., Duguay, C., Korhola, A., McNamara, J., Vincent, W.F., Vuglinsky, V., and Weyhenmeyer, GA. 2011. Arctic freshwater ece and its climatic role. Ambio 40:46–52. https://doi.org/10.1007/s13280-011-0214-9

Rantanen, M., Karpechko, A.Y., Lipponen, A., Nordling, K., Hyvärinen, O., Ruosteenoja, K., Vihma, T., and Laaksonen, A. 2022. The Arctic has warmed nearly four times faster than the globe since 1979. Communications Earth & Environment 3: 168. https://doi.org/10.1038/s43247-022-00498-3

Robinson, A.L., and Brown, LC. 2025. Simulated current and projected radiation balance of a High Arctic lake during the open water season. Arctic Science 11:1–22. https://doi.org/10.1139/as-2024-0081

Robinson, A.L., Ariano, S.S., and Brown, L.C. 2021. The Influence of snow and ice albedo towards improved lake ice simulations. Hydrology 8(1): 11. https://doi.org/10.3390/hydrology8010011

Serreze, M.C., and Barry, R.G. 2014. The Arctic climate system. Cambridge: Cambridge University Press.

Smith, P.A., Gilchrist, H.G., Forbes, M.R., Martin, J., and Allard, K., 2010. Inter-annual variation in the breeding chronology of Arctic shorebirds: Effects of weather, snow melt and predators. Journal of Avian Biology 41(3):292–304. https://doi.org/10.1111/j.1600-048X.2009.04815.x

Surdu, C.M., Duguay, C.R., and Prieto, D.F. 2016. Evidence of recent changes in the ice regime of lakes in the Canadian High Arctic from spaceborne satellite observations. The Cryosphere 10(3):941–960. https://doi.org/10.5194/tc-10-941-2016

Tom, M., Prabha, R., Wu, T., Baltsavias, E., Leal-Taixé, L., and Schindler, K. 2020. Ice monitoring in Swiss lakes from optical satellites and webcams using machine learning. Remote Sensing 12(21): 3555. https://doi.org/10.3390/rs12213555

Wang, X., Feng, L., Qi, W., Cai, X., Zheng, Y., Gibson, L., Tang, J., et al. 2022. Continuous loss of global lake ice across two centuries revealed by satellite observations and numerical modeling. Geophysical Research Letters 49(12): e2022GL099022. https://doi.org/10.1029/2022GL099022

Wu, Y., Duguay, C.R., and Xu, L. 2021. Assessment of machine learning classifiers for global lake ice cover mapping from MODIS TOA reflectance data. Remote Sensing of Environment 253: 112206. https://doi.org/10.1016/j.rse.2020.112206

Xiao, M., Rothermel, M., Tom, M., Galliani, S., Baltsavias, E., and Schindler, K. 2018. Lake ice monitoring with webcams. ISPRS Annals of the Photogrammetry, Remote Sensing and Spatial Information Sciences 4(2):311–317. https://doi.org/10.5194/isprs-annals-IV-2-311-2018

Young, K.L., and Labine, C. 2010. Summer hydroclimatology of an extensive low-gradient wetland: Polar Bear Pass, Bathurst Island, Nunavut, Canada. Hydrology Research 41(6):492–502. https://doi.org/10.2166/nh.2010.219

Young, K.L., and Brown, L.C. 2023. Temperature and precipitation trends of the shoulder seasons at Polar Bear Pass (Nanuit Itillinga) – A ramsar wetland of importance, Nunavut. Wetlands 43(68). https://doi.org/10.1007/s13157-023-01712-4

Young, K.L., Brown, L., and Labine, C. 2018. Snow cover variability at Polar Bear Pass, Nunavut. Arctic Science 4(4):669–690. https://doi.org/10.1139/as-2017-0016

Young, S.S. 2023. Global and regional snow cover decline: 2000–2022. Climate11(8): 162. https://doi.org/10.3390/cli11080162

Zhang, S., Pavelsky, T.M., Arp, C.D., Yang, X. 2021. Remote sensing of lake ice phenology in Alaska. Environmental Research Letters 16(6): 064007. https://doi.org/10.1088/1748-9326/abf965